

# Evaluation of Space-Time-Frequency (STF)-coded MIMO-OFDM Systems in Realistic Channel Models

Ricardo Kehrle Miranda<sup>a</sup>, João Paulo C. Lustosa da Costa<sup>a</sup>,

Marco A. M. Marinho<sup>a</sup>, Edison Pignaton de Freitas<sup>a,b</sup>, Rafael de Freitas Ramos<sup>a</sup>,

Kefei Liu<sup>c</sup>, Hing Cheung<sup>c</sup>, Leonardo Baltar<sup>d</sup> and Rafael Timóteo de Sousa Júnior<sup>a</sup>

Email: {rickehrle,jpdacosta}@unb.br, marco.marinho@ieee.org, edison.p.freitas@ufsm.br, rafaelframos@gmail.com, kefeilau@gmail.com, hcso@ee.cityu.edu.hk, leo.baltar@tum.de, desousa@unb.br

<sup>a</sup>Department of Electrical Engineering, University of Brasília, Brasília, Brazil

<sup>b</sup>Department of Applied Computing, Federal University of Santa Maria, Santa Maria, Brazil

<sup>c</sup>Department of Electronic Engineering, City University of Hong Kong, Kowloon, Hong Kong, China

<sup>d</sup>Munich University of Technology, Institute for Circuit Theory and Signal Processing, Munich, Germany

**Abstract**—By taking into account several dimension of the transmitted signal, such as space, frequency, period and time, MIMO-OFDM systems allow an increased spectral efficiency and an improved identifiability in comparison to matrix solutions. In this paper, we evaluate MIMO-OFDM systems for geometric scenarios where the narrow band approximation is violated. To this end a new data model is proposed to better represent the behavior of the system in the presence of wide band signals. Moreover, we also relax the assumption that the amount of transmitted antennas is equal to the number of transmitted symbols.

## I. INTRODUCTION

At the end of 2011, the amount of subscribers connected to mobile networks was close to 6 billions with an increasing rate of 0.6 billions per year. Moreover, high data rate applications are becoming more frequent. In order to fit such increasing demand, communication schemes that takes into account Multiple Input Multiple Output (MIMO) and Orthogonal Frequency Division Multiplexing (OFDM) solution at the same time can be applied [1]–[4].

Recently a new space-time-frequency diversity based MIMO-OFDM system has been proposed [4] where transmit signal design combines

frequency-domain Vandermonde spreading with a time-varying linear constellation pre-coding, while the received signal is formulated as a nested parallel factor (PARAFAC) model. Also, two extensions for this scheme were shown in [5].

In this paper we evaluate the performance of the MIMO-OFDM receivers proposed in [4] for geometric scenarios, i.e, simulation scenarios generated using ray tracing techniques instead of stochastic characteristics. These channels are generated using the Ilmprop software [7]. We formulate a mathematical representation for such scenarios and show, by means of simulations, that the narrow bands approximation is violated. The performance of two decomposition algorithms in both geometric and probabilistic channel is verified.

In [4], the amount of transmitted antennas is equal to the number of transmitted symbols. By employing the tensor representation, which offers greater identifiability, instead of the matrix representation we are able to relax this constraint to obtain increased data rates.

This remainder of this paper is organized as follows. In Section II, a data model is formulated as a nested PARAFAC model. This model is exploited for blind symbol decoding and channel estimation

as the channel model presented in Section II-C. In Section III, we show the proposed Least Squares Khatri-Rao Factorization (LS-KRF) receiver [4]. Numerical results are presented in Section IV. Finally, a conclusion is drawn in Section V.

*Notation:* Scalars are denoted by lower-case letters ( $a, b, \dots$ ), vectors are written as boldface lower-case letters ( $\mathbf{a}, \mathbf{b}, \dots$ ), matrices as boldface capitals ( $\mathbf{A}, \mathbf{B}, \dots$ ), and tensors as boldface calligraphic letters ( $\mathcal{A}, \mathcal{B}, \dots$ ). The superscripts  $\text{T}, \text{H}, \dagger$ , and  $*$  represent transpose, Hermitian transpose, pseudo-inverse and complex conjugate of a matrix, respectively. The  $\mathbf{A}(:, i) \in \mathbb{C}^{R \times 1}$  is a column vector denoting the  $i$ -th column of  $\mathbf{A} \in \mathbb{C}^{I \times R}$ . The operator  $\text{diag}(\mathbf{a})$  forms a diagonal matrix based on  $\mathbf{a}$ , and  $\text{vec}(\mathbf{A})$  yields an  $RI$ -dimensional vector that stacks the  $R$  columns of  $\mathbf{A} \in \mathbb{C}^{I \times R}$  on top of each other. The operator  $\text{vecdiag}(\mathbf{D})$  forms a vector  $\mathbf{d} \in \mathbb{C}^{R \times 1}$  from the diagonal elements of matrix  $\mathbf{D} \in \mathbb{C}^{R \times R}$ , while  $D_i(\mathbf{A})$  is a diagonal matrix constructed from the  $i$ -th row of  $\mathbf{A}$ . The  $\mathcal{T}_{(r)}$  is the  $r$ -mode matrix unfolding of  $\mathcal{T}$ .

Moreover, the Kronecker product and outer product operators are denoted by  $\otimes$  and  $\circ$ , respectively. The Khatri-Rao product between two matrices  $\mathbf{A} \in \mathbb{C}^{I \times R}$  and  $\mathbf{B} = [\mathbf{b}_1, \dots, \mathbf{b}_R] \in \mathbb{C}^{J \times R}$ , denoted by  $\diamond$ , is their column-wise Kronecker product

$$\mathbf{A} \diamond \mathbf{B} \doteq [\mathbf{A}(:, 1) \otimes \mathbf{B}(:, 1), \dots, \mathbf{A}(:, R) \otimes \mathbf{B}(:, R)]. \quad (1)$$

In this paper, the following property of the Khatri-Rao product is used

$$\mathbf{A} \text{diag}(\mathbf{x}^T) \mathbf{B}^T = (\mathbf{x}^T \diamond \mathbf{A}) \mathbf{B}^T, \quad (2)$$

where  $\mathbf{x}$  is an  $R$ -dimensional column vector.

## II. SYSTEM MODEL

### A. Transmitted Data

Consider a MIMO-OFDM wireless communication system employing  $Q$  transmit antennas and  $K$  receive antennas. In the frequency domain, information transmission is partitioned into groups of  $F$  neighboring sub-carriers and space-frequency coding is applied across these  $F$  sub-carriers. The transmission time-frame is composed of a collection of  $N$  short time-slots of  $P$  symbol periods each.

The information symbol stream is first parsed into symbol vectors  $\mathbf{s}_n \in \mathbb{C}^{M \times 1}$ . Each symbol vector is linearly pre-coded across  $P$  symbol periods by means of a set of unitary  $Q \times M$  space-time modulation matrices  $\{\mathbf{G}_1, \dots, \mathbf{G}_P\}$ . During the  $p$ -th symbol period,  $\mathbf{G}_p$  rotates the components of the symbol vector  $\mathbf{s}_n$  and loads a combination of these components into the  $Q$  transmit antennas. The pre-coded symbol vector is then used to modulate the  $F$  sub-carriers through a linear block-coding matrix  $\mathbf{W} \in \mathbb{C}^{F \times Q}$ . Along the same lines of [3], we choose  $\mathbf{W}$  as a Vandermonde matrix with the  $(f, q)$  entry given by

$$[\mathbf{W}]_{f,q} = e^{j(f-1)(q-1)\frac{2\pi}{Q}}. \quad (3)$$

Therefore, the space-frequency transmitted matrix at the  $p$ -th period and  $n$ -th time slot is given by

$$\mathbf{C}_{n,p} = \text{diag}(\mathbf{G}_p \mathbf{s}_n) \mathbf{W}^T \in \mathbb{C}^{Q \times F}, \quad (4)$$

where  $\mathbf{G}_p$  has the following form

$$\mathbf{G}_p = \Theta \text{diag}(\mathbf{a}_p) \in \mathbb{C}^{Q \times M}, \quad (5)$$

which  $\Theta \in \mathbb{C}^{Q \times M}$  being a discrete Fourier transform (DFT) matrix, and  $\mathbf{a}_p = [1, e^{j\phi}, \dots, e^{j(M-1)\phi}] \in \mathbb{C}^{1 \times M}$  is a phase rotation vector, with  $\phi$  being an elementary rotation that is randomly varied at the transmitter and can be optimized for a given  $Q$  and modulation type.

According to (3),  $\mathbf{G}_p$  is responsible for combining the symbols through different antennas while  $\mathbf{W}$  is responsible for combining the symbols through different frequencies, resulting in space-frequency coding. Note that in [4] the number of transmitted symbols  $M$  is equal to the number of antennas  $Q$ .

### B. Proposed Data Model

Assuming that the channel is constant over the whole time-frame, the discrete-time baseband equivalent model for the received signal is given by

$$\begin{aligned} \mathbf{Y}_{n,p} &= \sqrt{\frac{\rho}{Q}} \mathbf{H} \mathbf{C}_{n,p} + \mathbf{V}_{n,p} \\ &= \sqrt{\frac{\rho}{Q}} \mathbf{H} \text{diag}(\mathbf{G}_p \mathbf{s}_n) \mathbf{W}^T + \mathbf{V}_{n,p}, \end{aligned} \quad (6)$$

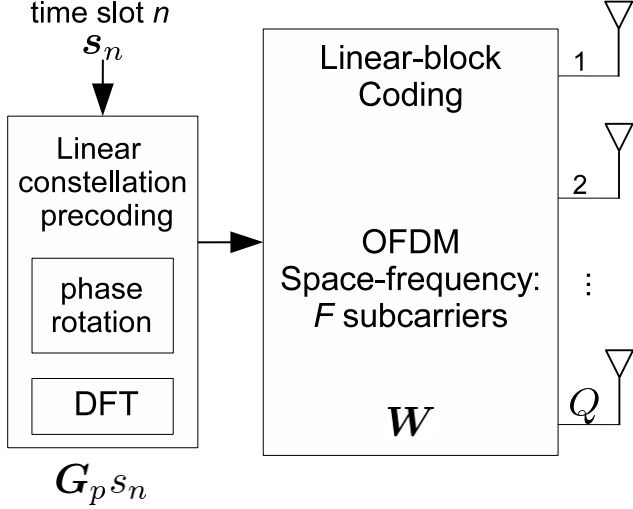


Fig. 1. MIMO-OFDM Transmitter

where  $\mathbf{Y}_{n,p} \in \mathbb{C}^{K \times F}$ , for  $n = 1, \dots, N$ , and  $p = 1, \dots, P$ , denotes the complex received signal matrix during the  $p$ -th symbol period of the  $n$ -th time-slot, and  $\mathbf{V}_{n,p}$  denotes zero-mean circularly symmetric complex Gaussian (ZMCSCG) noise. The channel matrix  $\mathbf{H}$  represents the channel gain for each transmitter-receiver antenna pair and  $\rho$  denotes the signal-to-noise ratio (SNR) at each receive antenna.

By concatenating all  $\mathbf{a}_p$  vectors into a matrix  $\mathbf{A}$  and all  $\mathbf{s}_n$  vectors into a matrix  $\mathbf{S}$ , (6) can be represented as

$$\mathbf{Y}_{n,p} = \sqrt{\frac{\rho}{Q}} \mathbf{H} \mathbf{D}_p (\mathbf{A} \mathbf{D}_n (\mathbf{S}) \mathbf{\Theta}^T) \mathbf{W}^T + \mathbf{V}_{n,p}. \quad (7)$$

By concatenating all  $P$  periods and all  $N$  time slots, we obtain the following matrix

$$\mathbf{Y} = \sqrt{\frac{\rho}{Q}} \left[ \left( \underline{(\mathbf{S} \diamond \mathbf{A}) \mathbf{\Theta}^T} \right) \diamond \mathbf{H} \right] \mathbf{W}^T + \mathbf{V}. \quad (8)$$

The signal part corresponds to the nested PARAFAC decomposition: the underlined part is the inner PARAFAC while the whole signal is the outer PARAFAC.

As presented in [4], the received signal can also be represented in tensor form with the inner part

being represented as

$$\mathcal{T} = \mathcal{I}_M \times_1 \mathbf{S} \times_2 \mathbf{A} \times_3 \mathbf{\Theta} \in \mathbb{C}^{N \times P \times Q}, \quad (9)$$

where  $\mathcal{I}_M$  represents the identity tensor of size  $M \times M \times M$  and  $\times_r$  for  $r = 1, \dots, R$ , is the  $r$ -mode product operator. Note that the 3rd dimension has size  $Q$ , differently from [4], where the number of transmitted symbols  $M$  was equal to the number of antennas  $Q$ .

Likewise (9), Equation (8) can be rewritten in tensor form as

$$\mathcal{Y} = \sqrt{\frac{\rho}{Q}} \cdot \mathcal{I}_M \times_1 \mathbf{H} \times_2 \mathbf{W} \times_3 \mathcal{T} + \mathcal{V} \in \mathbb{C}^{K \times F \times NP}, \quad (10)$$

where  $\mathcal{T} = [\mathcal{T}_{(3)}]^T$  and  $\mathcal{V}$  is the noise tensor.

The receiving process is summarized in Fig.2.

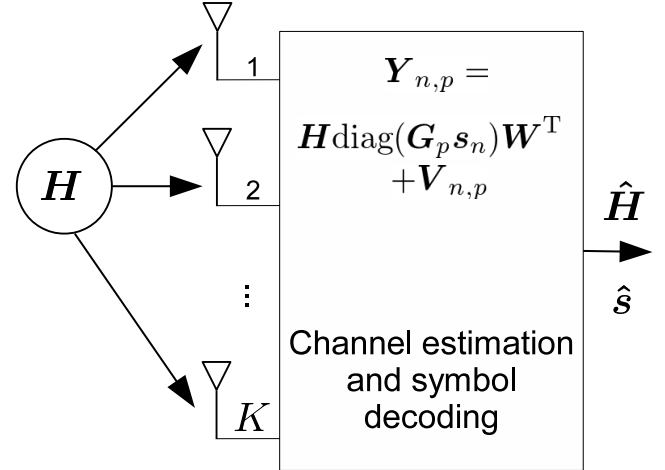


Fig. 2. MIMO-OFDM Receiver

### C. Proposed Geometric Channel

In order to evaluate the performance of the MIMO-OFDM system for more realistic scenarios, we apply the schemes presented on [4] to a specific geometric scenario corresponding to Figure 3. This scenario presents a line of sight (LOS) component depicted by a thick red line and two non-line-of-sight (NLOS) components depicted by thin black lines. The transmitter is equipped with a ULA composed of 3 antennas and the receiver with a ULA composed of 2 antennas.

Since, for wide-band transmissions, different frequency taps usually present different channel responses, we generalize (6) in order to get a more realistic model.

$$\mathbf{Y}_{n,p} = \sqrt{\frac{\rho}{Q}} [\mathbf{H}_1 \mathbf{C}_{n,p,1} | \dots | \mathbf{H}_F \mathbf{C}_{n,p,F}] + \mathbf{V}_{n,p}, \quad (11)$$

where the operator  $|$  stands for concatenation,  $\mathbf{H}_f \in \mathbb{C}^{K \times Q}$  is the channel for the  $f$ -th frequency component and  $\mathbf{C}_{n,p,f}$  is the  $f$ -th column of the matrix  $\mathbf{C}_{n,p}$ .

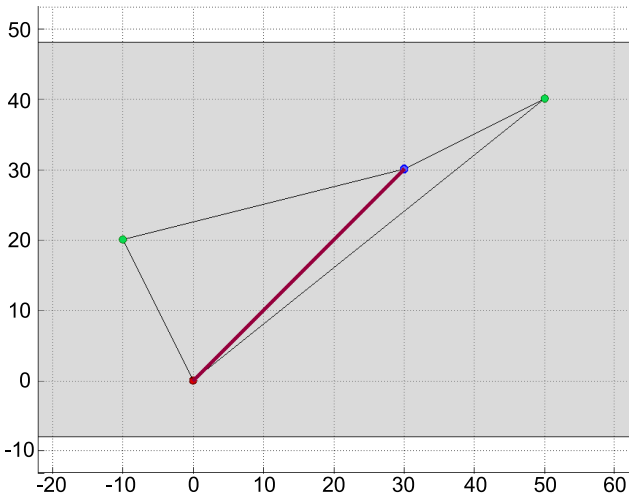


Fig. 3. Ilmprop scenario from above perspective with horizontal axes in meters

### III. LEAST SQUARES KHATRI-RAO FACTORIZATION (LS-KRF) BASED MIMO-OFDM RECEIVER

#### A. LS-KRF

Now we review the closed form LS-KRF based receiver [4] for semi-blind joint detection and channel estimation. First we estimate  $\mathbf{T}$  and  $\mathbf{H}$  via the outer PARAFAC model. The 2-mode unfolding of tensor  $\mathcal{Y}$  gives

$$[\mathcal{Y}]_2 = \mathbf{W} \cdot [(\mathbf{T} \diamond \mathbf{H})]^T. \quad (12)$$

After multiplying both sides in (12) by the pseudo-inverse of  $\mathbf{W}$  and then taking the transpose, we get

$$(\mathbf{T} \diamond \mathbf{H}) = (\mathbf{W}^\dagger \cdot [\mathcal{Y}]_2)^T \in \mathbb{C}^{NP \times K \times M}. \quad (13)$$

The unvectorization of the  $m$ -th column of  $(\mathbf{T} \diamond \mathbf{H})$ ,  $m = 1, \dots, M$ , yields a matrix  $\mathbf{Q}_m \in \mathbb{C}^{NP \times K}$ . According to (1), in the presence of noise,  $\mathbf{Q}_m$  is a rank-one matrix

$$\mathbf{Q}_m = \mathbf{H}(:, m) \circ \mathbf{T}_0(:, m). \quad (14)$$

Hence we can apply SVD to  $\mathbf{Q}_m$  to obtain the estimate  $\mathbf{H}(:, m) \in \mathbb{C}^{NP \times 1}$  and  $\mathbf{T}(:, m) \in \mathbb{C}^{K \times 1}$ . Suppose after SVD, we have

$$\mathbf{Q}_m = \mathbf{U}_m \cdot \Sigma_m \cdot \mathbf{V}_m^H, \quad (15)$$

then the estimates of  $\mathbf{H}(:, m)$  and  $\mathbf{T}(:, m)$  are given by

$$\hat{\mathbf{T}}(:, m) = \sqrt{\sigma_{1m}} \mathbf{U}_m(:, 1) \in \mathbb{C}^{NP \times 1} \quad (16)$$

and

$$\hat{\mathbf{H}}(:, m) = \sqrt{\sigma_{1m}} \mathbf{V}_m^*(:, 1) \in \mathbb{C}^{K \times 1}. \quad (17)$$

Similar with the ALS solution, the scaling ambiguity from  $\hat{\mathbf{T}}$  can be removed by knowing that the first row in  $\mathbf{T}$  is known.

## IV. SIMULATION RESULTS

In this section we analyze the performance of the proposed system for two different types of scenarios. A ‘‘close to typical rank’’ scenario is a scenario where the number of transmitted symbols  $M$  is large. The performance of the proposed system is also studied for geometric scenarios.

### A. Close to typical rank scenarios

In Figs. 4 and 5, we consider a MIMO-OFDM system with  $K = 4$  receive antennas,  $Q = 4$  transmit antennas,  $F = 8$  frequency bins,  $N = 10$  time slots, and  $P = 2$  periods. In both figures, we observe the performance of the ALS and LS-KRF by varying the SNR and  $M$ . For such configuration, note that the Kruskal’s condition for the outer PARAFAC is satisfied [4]. However, note that if  $M > Q$ , the Kruskal’s condition for the inner PARAFAC is not satisfied.

In Fig.4, the ALS completely fails when  $M > 4$ , since the Kruskal’s condition is not satisfied. However, for  $M \leq 4$ , the BER is zero for an SNR  $> 5$ .

In contrast to the ALS, the LS-KRF works partially even when  $M > 4$  as shown in Fig.5.

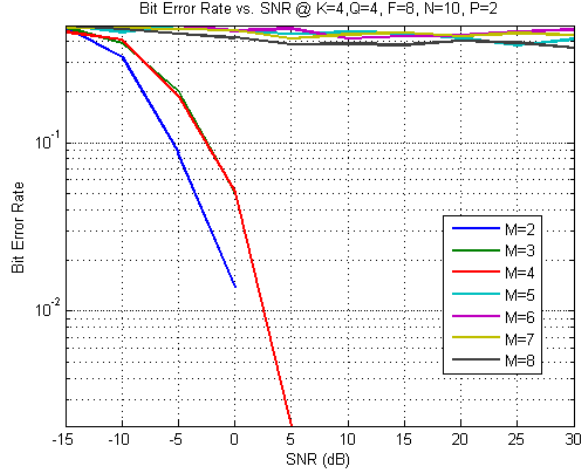


Fig. 4. Bit Error Rate vs SNR for the ALS with  $M = 2, 3, \dots, 8$ .

For  $M > 4$ , the BER varies from  $4 \cdot 10^{-2}$  until  $2 \cdot 10^{-1}$ . In Tab.1 we show the values of the BER versus  $M$  at SNR = 30 dB. The  $M(N - 1)$  column gives the number of transmitted symbols and  $M(N - 1)(1 - BER)$  gives the number of correctly received symbols. Even though the BER increases for great values of  $M$ , the amount of transmitted symbols also increases with the increase of  $M$ , verifying the advantage of using of the proposed model.

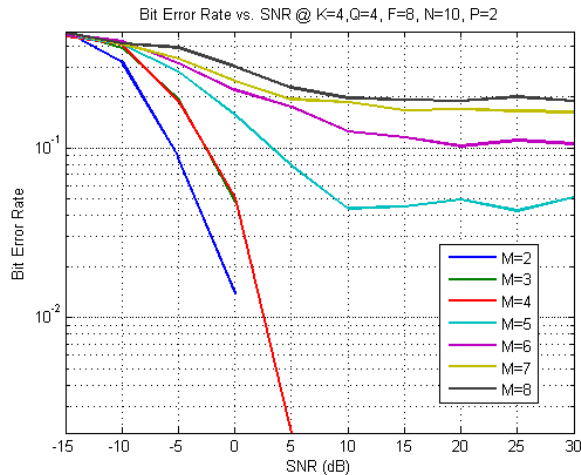


Fig. 5. Bit Error Rate vs SNR for the LS-KFR with  $M = 2, 3, \dots, 8$ .

TABLE I. EFFICIENCY FOR SNR = 30 dB, SECOND COLUMN: TRANSMITTED SYMBOLS. FOURTH COLUMN: CORRECTLY RECEIVED SYMBOLS

| $M$ | $M(N - 1)$ | BER   | $M(N - 1)(1 - BER)$ |
|-----|------------|-------|---------------------|
| 2   | 18         | 0     | 18                  |
| 3   | 27         | 0     | 27                  |
| 4   | 36         | 0     | 36                  |
| 5   | 45         | 0,1   | 40,5                |
| 6   | 54         | 0,125 | 47,25               |
| 7   | 63         | 0,2   | 50,4                |
| 8   | 72         | 0,2   | 57,6                |

### B. Geometric Channel

In this section we analyze geometric scenarios using our proposed expression (11). The MIMO-OFDM system has  $K = 2$  receive antennas,  $Q = 3$  transmit antennas,  $F = 100$  sub-carriers,  $P = 3$  periods, and  $N = 5$  time slots. In Fig.6, we divide a 40 MHz bandwidth into 800 sub-carriers and then select  $F = 100$  sub-carriers for our MIMO-OFDM system. We select the number of symbols  $M = 4$ , i.e., a number immediately larger than the Kruskal's condition limit. In this scenario, the better performance of the LS-KRF is clear as from -10dB.

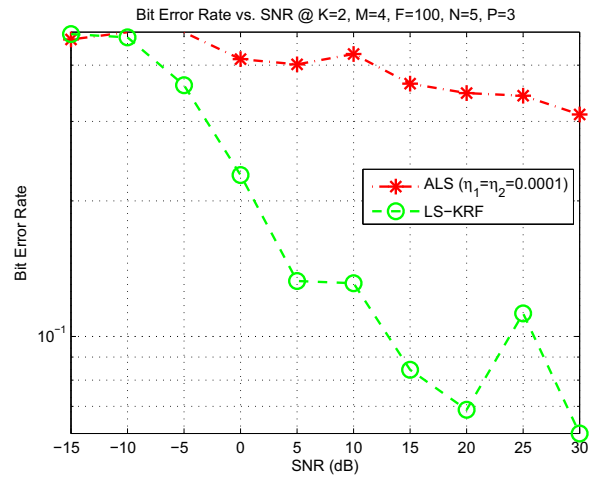


Fig. 6. Bit Error Rate vs SNR - 800 sub-carriers.

In Fig.7, we divide the 40 MHz bandwidth into 200 sub-carriers and we select the same quantity  $F = 100$  sub-carriers for our MIMO-OFDM system. This means that we are increasing the bandwidth of each sub-carrier, i.e., the narrow band approximation is violated and the performance is severely degraded. However, the LS-KRF still works partially for high SNR cases.

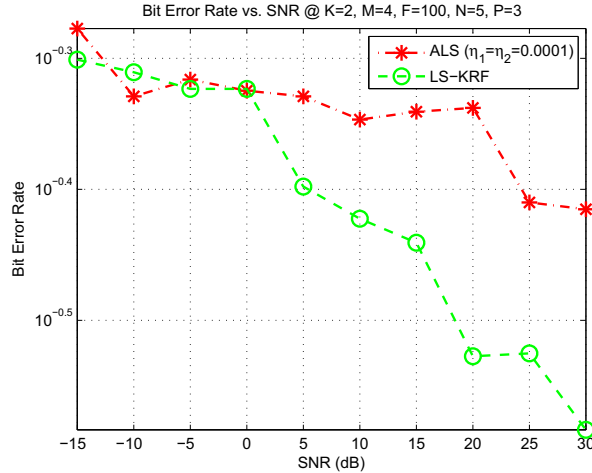


Fig. 7. Bit Error Rate vs SNR - 200 sub-carriers.

## V. CONCLUSIONS

In this paper a new data model for Space-Time-Frequency coded MIMO-OFDM systems was proposed. The proposed data model is also capable of eliminating the limitation of symmetric number of antennas being present at the transmitter and receiver. Due to this generalization, an increase in the data rate of the MIMO-OFDM technique is shown to be achievable. When the Kruskal's condition is violated the LS-KRF is still operational. Even with an increase in the BER, the increased number of transmitted symbols increases the amount of correctly received symbols. Also, the proposed data model is adequate for wide band scenarios.

As a future work, a scheme in which the Space-Time-Frequency coded MIMO-OFDM algorithms is adapted to wide band scenarios seems natural. However this task is not trivial. Once the channel is split into various linear channels the problem becomes bidimensional and the tensor algebra can no longer be applied. Using blind source separation schemes could be a way of recovering the data if the DFT and rotation matrix are carefully chosen so that the data distribution does not become gaussian.

## ACKNOWLEDGMENTS

This work was supported by the Brazilian Federal District Foundation for Research Support (FAPDF) and the Brazilian Ministry of Planning, Budget and Management and Research Support Agency of Rio Grande do Sul (FAPERGS).

## REFERENCES

- [1] A. L. F. de Almeida, G. Favier, and J. C. M. Mota, "Space-time multiplexing codes: A tensor modeling approach," in Proc. IEEE 7th Workshop Signal Processing Advances in Wireless Communications SPAWC'06, Cannes, France, July 2006, pp. 1–5.
- [2] A. L. F. de Almeida, G. Favier, and J. C. M. Mota, "A constrained factor decomposition with application to MIMO antenna systems," IEEE Trans. Signal Process., vol. 56, no. 6, pp. 2429–2442, 2008.
- [3] A. L. F. de Almeida, "Blind joint detection and channel estimation in space-frequency diversity systems using time-varying linear constellation precoding," in Brazilian Telecommunications Symposium (SBrT'11), Curitiba, Paraná, Brazil, October 2011.
- [4] K. Liu, J. P. C. L. da Costa, A. L. F. de Almeida and H. C. So, "A Closed Form Solution to Semi-Blind Joint Symbol and Channel Estimation in MIMO-OFDM Systems," in Proc. 2012 IEEE International Conference on Signal Processing, Communications and Computing (ICSPCC'12), Hong Kong, Aug. 2012.
- [5] K. Liu, J. P. C. L. da Costa, A. L. F. de Almeida, and H. C. So, "Semi-Blind Receivers for Joint Symbol and Channel Estimation in Space-Time-Frequency Diversity based MIMO-OFDM Systems," IEEE Transactions on Signal Processing
- [6] L. de Lathauwer, B. the Moor, J. Vanderwalle, "A multilinear singular value decomposition," SIAM, v. 21, n. 4, p. 1253–1278, 2000.
- [7] G. Del Galdo, M. Haardt and C. Schneider, "Geometry-based channel modeling in MIMO scenarios in comparison with channel sounder measurements," Advances in Radio Science - Kleinheubacher Berichte, v. 2, p. 117-126, 2004.